

High energy extragalactic multimessenger backgrounds from starburst and dead galaxies

Ellis R. Owen^{1,2*}, Yoshiyuki Inoue^{1,3,4}, Tatsuki Fujiwara¹ and Albert K. H. Kong⁵

¹*Theoretical Astrophysics, Department of Earth and Space Science,
Graduate School of Science, The University of Osaka,
Toyonaka 560-0043, Osaka, Japan*

²*Astrophysical Big Bang Laboratory (ABBL), RIKEN Pioneering Research Institute,
Wakō, Saitama, 351-0198 Japan*

³*Kavli Institute for the Physics and Mathematics of the Universe (WPI),
UTIAS, The University of Tokyo, Kashiwa, Chiba 277-8583, Japan*

⁴*Interdisciplinary Theoretical & Mathematical Science Program (iTHEMS),
RIKEN, 2-1 Hirosawa, Saitama 351-0198, Japan*

⁵*Institute of Astronomy, National Tsing Hua University,
No. 101, Section 2, Kuang-Fu Rd, Hsinchu 30013, Taiwan (ROC)*

Abstract. Starburst galaxies are γ -ray sources. Canonically, their emission is driven by hadronic cosmic rays (CRs) interacting with interstellar gas, forming γ -rays via the decay of neutral pions. Charged pions are also formed in this process. They decay into secondary leptons, including electrons and neutrinos. Starburst galaxies are therefore also expected to be neutrino sources, and their high-energy γ -ray emission may include a secondary leptonic component. Leptonic γ -rays may also originate from electrons directly energized by shocks within the interstellar medium of galaxies, or from pulsars and their surrounding halos. In the Milky Way, pulsars/pulsar halos are the dominant γ -ray source class. They are associated with stellar remnants or old stellar populations, and are presumably abundant in old galaxies. In this work, we show that the collective high-energy emission from galaxies can account for only a fraction of extragalactic neutrinos, but can form a major component of the extragalactic γ -ray background. Contrary to the traditional view, a substantial fraction of this radiation may originate from leptonic processes, including from old, quiescent galaxies.

Key words: Cosmic rays - γ -rays - neutrinos - galaxies - millisecond pulsars/halos

1. Introduction

Recent advances in the past decade have greatly improved our understanding of the origins of high-energy photons and particles from beyond our galaxy. Key developments include new measurements of the

*Speaker

diffuse neutrino flux by IceCube, spanning 30 TeV to PeV energies (IceCube Collaboration, 2013; Aartsen et al., 2016, 2020), and the extragalactic γ -ray background observed by *Fermi*-LAT (Ackermann et al., 2015). These backgrounds can be decomposed into two components: one arising from emission by resolved, individual extragalactic sources, and another from the combined emission of all unresolved sources across the observable Universe. The unresolved component is believed to predominantly originate from populations of distant, point-like sources that cannot be individually detected (Ackermann et al., 2015). These include objects such as blazars (e.g. Inoue and Totani, 2009), radio galaxies (e.g. Inoue, 2011; Stecker et al., 2019) and starburst galaxies (e.g. Roth et al., 2021; Chen and Totani, 2025).

Starburst galaxies are cosmic ray (CR) reservoirs, with CRs mainly supplied by the end-products of stellar evolution, such as supernova remnants. Their interstellar conditions allow them to operate effectively as calorimeters, efficiently converting their CR supply into high energy γ -rays and neutrinos. This makes them well-motivated candidates for the diffuse extragalactic background flux, with nearby starburst galaxies found to be γ -ray bright (Ajello et al., 2020). The contribution from starburst galaxies has been estimated to account for a significant fraction of the extragalactic γ -ray background and, in some model configurations, may even saturate it (Roth et al., 2021). While their role in producing the extragalactic neutrino flux is likely to be less substantial, detailed spectral modeling variations may allow for higher contributions. Observations have also revealed γ -ray emission from nearby quiescent galaxies, such as M31 (Ajello et al., 2020). In these systems, the emission may be linked to evolved stellar populations and their compact high-energy sources, including millisecond pulsars (MSPs) and TeV γ -ray-emitting pulsar halos. These sources could also contribute to the high-energy γ -ray background (Xu and Hooper, 2022).

In this work, we present a new determination of the multimessenger high-energy emission from galaxies to systematically investigate the combined origins of the extragalactic γ -ray and neutrino backgrounds from galaxies. Compared to previous studies, our approach extends beyond starbursts to include main-sequence and quiescent galaxies. This allows for a more robust assessment of the high-energy emission originating from diverse galaxy types over a broad range of redshifts.

2. Cosmic rays in galaxies

2.1. PROPAGATION AND CONFINEMENT

CRs are typically energized within galaxies by shocks and turbulence. These are often driven by star-formation activities through feedback from supernovae (SNe) and winds. We therefore parameterize the CR supply rate within a galaxy using its SN event rate, and adopt a power-law injection spectrum with an index of -2.1, and an exponential cut-off of 50 PeV. 2 per-cent of the total CR energy is supplied to relativistic electrons, with the remaining fraction supplied to protons. Once energized, CRs diffuse through turbulent interstellar magnetic fields. They then slowly leak out of a galaxy or are attenuated by particle interactions. To account for CR propagation and losses, we adopt the model introduced by Owen et al. (2019). This invokes an interstellar medium (ISM) permeated by Kraichnan-type magnetic turbulence, where the magnetic energy density is set to be the same as the energy supplied by SNe over an advection timescale (this is similar to the approach adopted by Chen and Totani, 2025).¹

2.2. INTERACTIONS AND MULTIMESSENGER EMISSION SIGNATURES

Above a threshold energy of ~ 280 MeV, hadronic CRs interact with ambient gas to produce charged and neutral pions. These pions decay, producing γ -rays, neutrinos and secondary electrons and positrons (hereafter, we do not distinguish between electrons and positrons). We model the production of these secondary particles using *Aafrag* 2.01 (Kachelrieß et al., 2023). This approach allows the direct computation of the pion decay γ -ray and neutrino spectra for a given galaxy. Hadronic interactions attenuate the primary CR flux within galaxies. This attenuation is accounted for self-consistently in our adopted CR distribution model (Owen et al., 2019). Additional γ -ray emission arises from bremsstrahlung and inverse Compton scattering of CR electrons within a galaxy. In our calculations, we include contributions from both primary CR electrons and secondary electrons produced in hadronic collisions. To compute this emission, we consider that the electron distribution is held at a steady state where particle injection is balanced by cooling through radiative and collisional processes. In our model, both hadronic and leptonic losses, as well as their associated emission, depend on

¹An adjustment is made to ensure our model reproduces the magnetic field strength of the Galactic ISM for parameter values appropriate for the Milky Way.

several key factors: magnetic field strength, gas density, and the intensity of the interstellar radiation field. These quantities are parameterized using the star formation rate.

3. Pulsar populations in galaxies

Pulsars and their surrounding halos are the dominant γ -ray source class in our Galaxy (for a recent review, see López-Coto et al., 2022), and are considered capable of driving most of the >500 GeV emission from other similar main-sequence galaxies, including M31 (Xu and Hooper, 2022). They are separated into two distinct populations based on their spin-down properties. The majority are canonical pulsars, which can host spatially-extended ‘pulsar halos’ observed in TeV γ -rays. Pulsar halos are predominantly leptonic, diffusion-dominated systems that typically feature an extended region where CR diffusion is suppressed compared to the ISM average (e.g. Schroer et al., 2023). We construct a simplified pulsar halo spectral model using a single suppressed, uniform diffusion coefficient (reduced by a factor of 10 relative to typical ISM values) and a power-law CR injection spectrum with an exponential cutoff at 1 TeV and index of -1.6, gauged empirically from the spectrum of the Geminga pulsar halo when adopting a steady-state balance between electron injection and radiative cooling. We adopt this spectral model as a baseline for the combined emission from a population of pulsar halos in a galaxy, parameterized by their time-evolving spin-down rates.

We construct a population model to describe the evolution of pulsar halos in a galaxy. This considers that the population of pulsar halos at a given time in a galaxy can be characterized in terms of their birth rate, death rate, and spin-down rate, where the emission properties of each pulsar halo are parameterized by its spin-down luminosity. The number of pulsar halos in a galaxy with luminosities between L_γ and $L_\gamma + dL_\gamma$ is $n_{\text{ph}}(L_\gamma, t)dL_\gamma$. The evolution of the halo population’s luminosity function is then:

$$\frac{\partial n_{\text{ph}}(L_\gamma, t)}{\partial t} + \frac{dL_\gamma}{dt} \frac{\partial n_{\text{ph}}(L_\gamma, t)}{\partial L_\gamma} = -\kappa n_{\text{ph}}(L_\gamma, t) + f_{\text{ph}}(L_\gamma, t), \quad (1)$$

where κ represents their ‘death’ rate, $f_{\text{ph}}(L_\gamma, t)$ is the formation rate, and dL_γ/dt represents their fading, brightening, or possible re-brightening.

The pulsar ‘birth’ term is regulated by the SN event rate of a galaxy, with a fraction of SN events producing pulsar and halo systems. For the

intrinsic birth luminosity function, we adopt a power-law distribution, which has been shown to accurately represent the initial spin-down (and hence luminosity) distribution of the γ -ray and radio pulsar populations in the Milky Way (see Watters and Romani, 2011). The fading of pulsar halos over time is modeled by tracking the evolution of the spin-down luminosity of their parent pulsars. The halo death rate is modeled using a characteristic death timescale. This is derived from the empirical pulsar ‘death line’, considered to represent the threshold for sustaining electron-positron pair production within the pulsar’s magnetosphere.

The second population are MSPs. These are recycled systems originating from evolved compact binaries that have been spun-up through past accretion episodes or dynamical interactions (Alpar et al., 1982; Hui et al., 2010). The γ -ray spectrum of MSPs is similar to that of normal pulsars. As a characteristic MSP spectral model, we adopt a log-parabola with parameter values fit by Lloyd et al. (2024) for the stacked emission from 118 *Fermi*-detected MSPs. We do not include a halo component in the spectrum. The MSP population is modeled in a similar way to the pulsar halos, characterized in terms of their birth and death rates in a galaxy, and their ageing (fading).

While the death condition for MSPs is the same as that for canonical pulsars, their far lower spin-down rate results in a relatively constant γ -ray luminosity over Gyr timescales so that the fading term in our MSP population model is negligible. MSP formation depends on a spin-up accretion process or dynamical interactions, indicating that these systems form as binaries (Alpar et al., 1982) or in regions of high stellar densities (e.g., Hui et al., 2010). The birth rate of MSPs $f_{\text{msp}}(L_\gamma, t)$ is therefore set by the number of SN events from a fraction of progenitor stars which have sufficient mass to yield a neutron star, and is then scaled by the relative frequency of dynamical encounters. The evolution of a population of MSPs in our model is then described by:

$$\frac{dn_{\text{msp}}(L_\gamma, t)}{dt} = -\kappa n_{\text{msp}}(L_\gamma, t) + f_{\text{msp}}(L_\gamma, t) . \quad (2)$$

(see also Wu, 2001). By directly integrating this equation and assuming (1) there are initially no MSPs, and (2) the MSP death timescale is much longer than the evolutionary timescale of a galaxy, the result reduces to a time-independent luminosity function, $n_{\text{msp}}(L_\gamma) \approx f_{\text{msp}}^0(L_\gamma) M_*$, where M_*

is the stellar mass of a galaxy and $f_{\text{mSP}}^0(L_\gamma)$ is the initial MSP luminosity function normalized to the formation rate of MSPs per stellar mass.² We model $n_{\text{mSP}}(L_\gamma)$ using a broken power-law with best-fit parameters from Bartels et al. (2018).

4. Multimessenger emission from galaxies

4.1. PROTOTYPE GALAXY MODEL

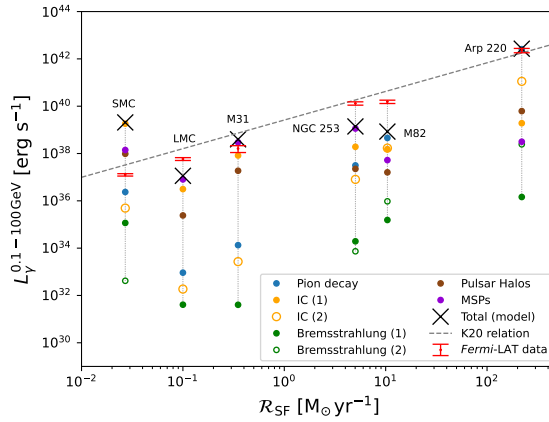


Figure 1: Relationship between 0.1-100 GeV γ -ray luminosity and star-formation rate for six nearby galaxies. Total γ -ray luminosities are shown by red (observed) and black (model predicted) crosses. Contributions from different emission components are indicated by circles, with emission associated with primary (1) / secondary (2) CRs indicated by filled / open circles. The empirical relation of Kornecki et al. (2020) is shown in gray (K20).

By parameterizing the emission models described in Sections 2 and 3, we construct a prototype model for the multimessenger high-energy emission from a galaxy. The model is specified by four inputs: a galaxy’s effective radius, stellar mass, star-formation rate, and redshift. Other parameters, such as CR spectral properties, are either fixed or derived from these inputs. We validate our model against the spectra of six nearby galaxies where the γ -ray emission is believed to be dominated by CR activity associated with their stellar populations (Ajello et al., 2020). Without detailed fitting, our model predictions show reasonable agreement with these

²This is estimated from a binary formation rate of 0.7 (see Duchêne and Kraus, 2013, for a review of multiplicities of massive stars) and enhanced by the average stellar interaction rate (given by the square of the stellar density; see e.g. Hui et al. 2010).

observations. Some differences emerge in the predicted total 0.1-100 GeV γ -ray luminosities when compared to *Fermi*-LAT data, as shown in Figure 1. These are primarily driven by variations in the galactic magnetic field, which may include components not accounted for in our model. Both CR confinement and inverse Compton emission (which is particularly sensitive to the efficiency of electron synchrotron cooling) are influenced by the magnetic field. Despite these differences, our model reproduces the empirical trend (K20), indicating that it is able to capture the overall behavior of γ -ray emission across a population of galaxies.

4.2. GALAXY POPULATION MODEL

We adopt the empirical semi-analytic galaxy-halo connection simulation, **UniverseMachine** (Behroozi et al., 2019) as a galaxy population model. This provides a self-consistent view of galaxies' star formation rates, stellar masses, host halo properties, assembly histories, and redshifts. It is constrained by empirical quantities, including galaxies' observed stellar mass functions, star-formation rates, quenched fractions, ultraviolet (UV) luminosity functions, UV-stellar mass relations and the environmental dependence of quenching. These empirical constraints ensure that **UniverseMachine** offers a robust baseline model, calibrated against the real Universe.

4.3. MULTIMESSENGER BACKGROUNDS

We post-process the **UniverseMachine** outputs with our galaxy prototype model to calculate the combined γ -ray and all-flavor neutrino emission from galaxy populations. Using a cosmological radiative/particle transfer formulation, we determine the flux arriving at Earth, ensuring conservation of the phase-space density of photons and neutrinos in an evolving cosmology. We integrate over all galaxies within the redshift range from $z=0$ to 6, beyond which their flux contribution becomes negligible. Our calculations account for the attenuation and cascade reprocessing of high-energy γ -rays through pair-production interactions with intergalactic radiation fields. These include the cosmic microwave background (CMB) and the extragalactic background light (EBL; adopting the model of Saldana-Lopez et al. 2021). Figure 2 presents our results for the total γ -ray and all-flavor neutrino emission contributions from galaxies.

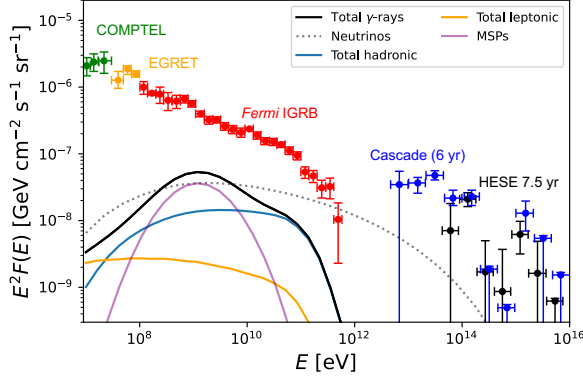


Figure 2: Galaxy contributions to the diffuse extragalactic γ -ray and all-flavor neutrino flux, compared with observational data from *COMPTEL* (Kappadath et al., 1996), *EGRET* (Sreekumar et al., 1998), *Fermi*-LAT (Ackermann et al., 2015) and IceCube (IceCube Collaboration, 2013; Aartsen et al., 2016, 2020). The total predicted contributions are shown in black, as labeled. The γ -ray flux is comprised of a mix of MSP emission, pion decays, and a sub-dominant leptonic inverse Compton component (attributed mainly to secondary CR electrons).

5. Remarks and conclusions

We find that most of the neutrinos in our model originate from CR interactions in strongly starbursting galaxies. However, our calculations indicate that it is unlikely these CR processes in galaxies alone could saturate the neutrino flux under any plausible model configuration. Instead, much of the remaining observed neutrino flux likely originates in other environments, e.g. blazars and Seyfert galaxies.

Our calculations also show that the γ -ray emission from CR processes in galaxies likely represents a non-negligible component of the extragalactic γ -ray background. In contrast to some previous works (e.g. Roth et al., 2021), our results suggest that galaxies do not saturate the γ -ray background at any energy. However, they may still contribute a substantial component of the flux at energies above a few tens of GeV up to 1 TeV. We also confirm the presence of a leptonic γ -ray emission component from galaxies at energies below ~ 0.1 GeV reported by previous studies (e.g. Roth et al., 2021; Chen and Totani, 2025), and additionally find that quiescent ‘dead’ galaxies with old stellar populations could contribute substantial GeV γ -ray emission Gyrs after their main star-formation activity. This introduces evolved galaxies as a potential source population in the GeV γ -ray sky

that has not previously been widely considered. Their contribution at these energies could be comparable to, or even exceed, that of starburst galaxies and is strongly dominated by MSP populations. This may naturally explain a spectral excess seen in *Fermi* data at around 1 GeV.

Acknowledgements: E.R.O is an international research fellow under the Postdoctoral Fellowship of the Japan Society for the Promotion of Science (JSPS), supported by JSPS KAKENHI Grant Number JP22F22327, and also acknowledges support from the RIKEN Special Postdoctoral Researcher Program for junior scientists. Y.I. is supported by an NAOJ ALMA Scientific Research Grant 2021-17A, JSPS KAKENHI Grants JP18H05458, JP19K14772, and JP22K18277, and the World Premier International Research Center Initiative (WPI), MEXT, Japan. This work was partially supported by the joint research program of the Institute for Cosmic Ray Research, the University of Tokyo. Numerical computations were carried out on the Cray XC50 supercomputer at the Center for Computational Astrophysics, National Astronomical Observatory of Japan and at the Yukawa Institute Computer Facility, Kyoto University. We thank Dr. Alison Mitchell for providing a helpful and constructive review that improved this article.

References

- Aartsen et al. (2016). Observation and Characterization of a Cosmic Muon Neutrino Flux from the Northern Hemisphere Using Six Years of IceCube Data. *Astrophys. J.*, 833(1):3.
- Aartsen et al. (2020). Characteristics of the Diffuse Astrophysical Electron and Tau Neutrino Flux with Six Years of IceCube High Energy Cascade Data. *Phys. Rev. Lett.*, 125(12):121104.
- Ackermann et al. (2015). The Spectrum of Isotropic Diffuse Gamma-Ray Emission between 100 MeV and 820 GeV. *Astrophys. J.*, 799(1):86.
- Ajello et al. (2020). The γ -Ray Emission of Star-forming Galaxies. *Astrophys. J.*, 894(2):88.
- Alpar et al. (1982). A new class of radio pulsars. *Nature*, 300(5894):728–730.
- Bartels et al. (2018). Bayesian model comparison and analysis of the Galactic disc population of gamma-ray millisecond pulsars. *MNRAS*, 481(3):3966–3987.
- Behroozi et al. (2019). UniverseMachine: The correlation between galaxy growth and dark matter halo assembly from $z = 0-10$. *MNRAS*, 488(3):3143–3194.
- Chen et al. (2025). The diffuse extragalactic gamma-ray background radiation: star-forming galaxies are not the dominant component. *arXiv e-prints*, page arXiv:2502.19879.
- Duchêne et al. (2013). Stellar Multiplicity. *Ann. Rev. Astron. Astrophys.*, 51(1):269–310.
- Hui et al. (2010). Dynamical Formation of Millisecond Pulsars in Globular Clusters. *Astrophys. J.*, 714(2):1149–1154.

- IceCube Collaboration (2013). Evidence for High-Energy Extraterrestrial Neutrinos at the IceCube Detector. *Science*, 342(6161):1242856.
- Inoue (2011). Contribution of Gamma-Ray-loud Radio Galaxies' Core Emissions to the Cosmic MeV and GeV Gamma-Ray Background Radiation. *Astrophys. J.*, 733(1):66.
- Inoue et al. (2009). The Blazar Sequence and the Cosmic Gamma-ray Background Radiation in the Fermi Era. *Astrophys. J.*, 702(1):523–536.
- Kachelrieß et al. (2023). AAfrag 2.01: interpolation routines for Monte Carlo results on secondary production including light antinuclei in hadronic interactions. *Computer Physics Communications*, 287:108698.
- Kappadath et al. (1996). The preliminary cosmic diffuse γ -ray spectrum from 800keV to 30MeV measured with COMPTEL. *Astron. Astrophys., Suppl. Ser.*, 120:619–622.
- Kornecki et al. (2020). γ -ray/infrared luminosity correlation of star-forming galaxies. *Astron. Astrophys.*, 641:A147.
- Lloyd et al. (2024). The effect of pulsar geometry on the observed gamma-ray spectrum of millisecond pulsars. *MNRAS*, 530(4):3552–3569.
- López-Coto et al. (2022). Gamma-ray haloes around pulsars as the key to understanding cosmic-ray transport in the Galaxy. *Nat. Astron.*, 6:199–206.
- Owen et al. (2019). Starburst and post-starburst high-redshift protogalaxies. The feedback impact of high energy cosmic rays. *Astron. Astrophys.*, 626:A85.
- Roth et al. (2021). The diffuse γ -ray background is dominated by star-forming galaxies. *Nature*, 597(7876):341–344.
- Saldana-Lopez et al. (2021). An observational determination of the evolving extragalactic background light from the multiwavelength HST/CANDELS survey in the Fermi and CTA era. *MNRAS*, 507(4):5144–5160.
- Schroer et al. (2023). TeV halos and the role of pulsar wind nebulae as sources of cosmic-ray positrons. *Phys. Rev. D*, 107(12):123020.
- Sreekumar et al. (1998). EGRET Observations of the Extragalactic Gamma-Ray Emission. *Astrophys. J.*, 494(2):523–534.
- Stecker et al. (2019). The Extragalactic Gamma-Ray Background from Core-dominated Radio Galaxies. *Astrophys. J.*, 879(2):68.
- Watters et al. (2011). The Galactic Population of Young γ -ray Pulsars. *Astrophys. J.*, 727(2):123.
- Wu (2001). Populations of X-ray Binaries and the Dynamical History of Their Host Galaxies. *Publ. Astron. Soc. Aust.*, 18(4):443–450.
- Xu et al. (2022). Contribution from TeV halos to the isotropic gamma-ray background. *Phys. Rev. D*, 106(2):023005.